
Characterisation of impact response of metallic foam/ceramic laminates

A. E. Markaki and T. W. Clyne

The impact response of laminated composites consisting of alternate layers of Al alloy foam and Al₂O₃ was studied experimentally in low and intermediate velocity regimes. Low velocity impacts (1.2–2.8 m s⁻¹) were conducted using an instrumented falling weight apparatus and were compared with static indentation tests (0.2 × 10⁻⁴ m s⁻¹). Intermediate velocity impacts were carried out by means of both Hopkinson bar (60 m s⁻¹) and gas gun (200 m s⁻¹) tests. Post-impact damage was assessed using X-ray radiography and microscopy. It was found that there is good correlation between low velocity impact and quasi-static responses. In both cases, penetration of the layered targets resulted in the formation of a distinctive plug. Increasing impact velocity (intermediate velocity range) switched the penetration mode from plugging to fragmentation, giving rise to an increase in the absorbed energy. In this range, impacts led to localisation of damage in the region under the projectile. Furthermore, a comparison has been made between the penetration response of foam laminates and dense metal laminates of equivalent areal density. Preliminary results suggest that the dense metal laminates are superseded by the foam laminates on an energy absorption basis.

MST/4575

The authors are in the Department of Materials Science and Metallurgy, University of Cambridge, Pembroke Street, Cambridge CB2 3QZ, UK. Contribution to 'Metal matrix composites VII' (MMC VII) held at The Institute of Materials in London on 8–9 December 1999.

© 2000 IoM Communications Ltd.

Introduction

Metallic foams tend to behave in a brittle manner under tensile stresses and, as a result of this, mechanical exploitation is oriented towards loading configurations that involve compression. When metallic foams are subjected to compressive loads, plastic buckling and bending of the cell walls takes place in a progressive fashion, which can lead to high energy absorption. The potential for large plastic strains makes metallic foams ideal energy absorbers, since a limit can be set on the level of the force transmitted. The demand for achieving low weight structures while exhibiting better performance has led the way for non-metallic materials such as ceramics to be used. When combining these two materials in a layered arrangement, ceramic layers will be responsible for carrying the majority of load and also for performing the important task of spreading out the contact force, whereas the foam layers are expected to absorb impact energy by progressive deformation. Although the energy expended in fracturing ceramics is very low (a few tens of joules per metre squared), their presence is found to be important in deflecting foreign objects providing there is sufficiently strong backing by a ductile medium.^{1–4} By tailoring the foam and ceramic materials and the layer thicknesses, it may be possible to produce structures with improved impact resistance. Because there have been virtually no studies hitherto on the impact response of metallic foam/ceramic laminates, it is essential to understand the deformation mechanisms involved in order to facilitate the design of structures with optimised impact performance.

In the present study, the impact failure of an Al alloy foam/Al₂O₃ layered composite has been investigated. For this purpose, three types of relatively high speed testing were employed including the falling weight test, the split Hopkinson pressure bar (SHPB), and a gas gun test. The first type simulates low velocity impact. The laminates were subjected to different impact velocities, producing increasing damage up to penetration. The other two types of test represent intermediate velocity impacts. The laminates were impacted with energies well above the

threshold for penetration. The induced damage and the energy absorbed at different impact velocities were compared.

Experimental procedure

MATERIALS AND LAMINATE FABRICATION

Laminates consisting of a total of seven alternate layers of Al₂O₃ and Al alloy foam were fabricated by hot pressing, with the Al₂O₃ layers arranged on the outside. Two nominal foam layer thicknesses h_f of about 2 and 3 mm were considered, while the Al₂O₃ layers were of a constant thickness ($h_c = 1$ mm).

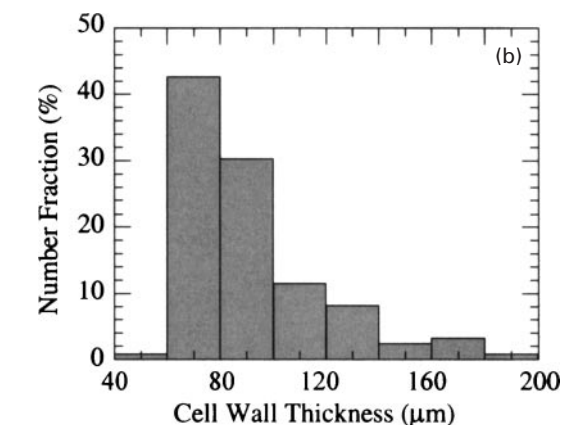
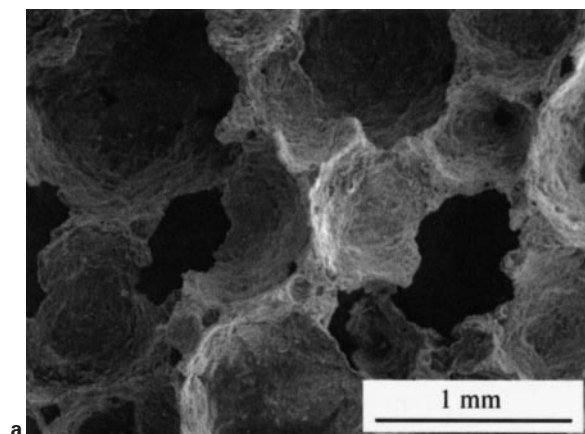
The foam was made from an Al–12Si–0.6Mg casting alloy via a powder metallurgy route.⁵ As illustrated in Fig. 1a, Al–12Si–0.6Mg foam has a predominantly closed cell structure. The cell wall thickness distribution is shown in Fig. 1b. Important parameters for the powder-route foam are summarised in Table 1.

IMPACT AND STATIC TESTING

Square specimens with a side length of 60 mm were cut from the bonded plates using a diamond wafering blade. The specimens produced had an areal density in the range 19–24 kg m⁻². The laminates were firmly fixed at all edges using annular clamps of 40 and 60 mm internal and external diameter, respectively.

Falling weight

Low velocity impact tests were carried out using an instrumented falling weight apparatus. The system consists of a hemispherical tipped impactor attached to a crosshead. Steel tups with a diameter of 10 mm and a mass of 75 g were used for all tests. The impactor was instrumented with a strain-gauged 5 kN load cell to provide the force–time history. A timer triggered by a pair of light gates was used to measure the impact velocity just before impact. From the time interval required for the trigger to travel between the

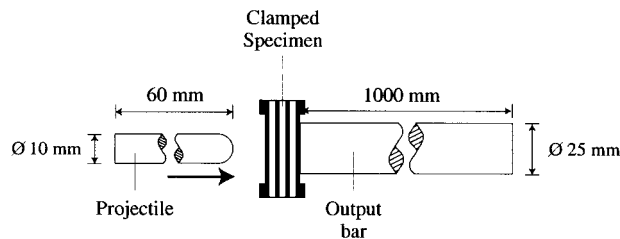


1 a typical cell structure of Al-12Si-0.6Mg foam and b cell wall thickness distribution: average cell wall thickness ~90 µm

two time sensors and the distance between them, the initial impact velocity could be calculated. During the tests, the weight (2.63 kg) was kept constant, while the drop height was varied, producing impact velocities in the range 1–3 m s⁻¹ (the incident impact energy was 2–10 J). After the first impact, the impactor was captured, to avoid further damage owing to secondary strikes. The impact force and duration were recorded by a data acquisition system, which had an output sampling interval of 10 µs.

Split Hopkinson pressure bar

Impact tests were performed using a split Hopkinson pressure bar (SHPB). The system consists of a hemispherical tipped impactor and an output bar, as shown schematically in Fig. 2. The output bar, made of high strength steel, fits into a slot machined into the base of the specimen mount. A high pressure air gun launches sabots carrying the projectiles. The projectiles, made of the same material as the output bar, had a nominal weight of 36 g. The striking velocity, measured from the transit time between two light beams spaced 50 mm apart, was



2 Experimental set-up for Hopkinson bar tests

~60 m s⁻¹. As the projectile struck the specimen, a compressive longitudinal wave was transmitted through the specimen to the output bar. Strain gauges mounted on the surface of the output bar allowed the stress waves to be analysed. The data were recorded at time increments of 0.5 µs. Tests were also carried out with the laminates resting on a 10 mm thick hardened steel plate to eliminate any flexural effects.

Gas gun

Higher velocities were achieved using a nitrogen pressurised gas gun. In these tests, the impact performance of the target materials was characterised by computing the loss of kinetic energy of the projectile during impact. By measuring the projectile velocity before penetration (striking velocity V_s) and after penetration of the target (residual velocity V_r), the energy absorbed by the laminates can be calculated using the formula

$$m(V_s^2 - V_r^2)/2 \dots \dots \dots (1)$$

where m is the projectile mass. The projectiles, mounted in the sabots, were fired from a 50 mm bore cartridge gun. The front face of the sabot was covered with a piece of brass shim in order to make contact with two shorting pins mounted at the muzzle end, 50 mm apart. The signals generated by the sabot passage allowed determination of the striking velocity, which was measured to be ~200 m s⁻¹. Subsequently, a sabot stripper plate was used to separate the projectile from the sabot, before hitting the target. The residual velocity was measured by signals obtained from the transit time between two foil screens spaced 200 mm apart. The first screen was 100 mm behind the rear face of the target. Each foil screen consisted of a sheet of A4 paper sandwiched between two aluminium foil sheets. The piercing of each screen by the conducting projectile produced a short circuit, which was detected using a data acquisition system. The data were recorded at time intervals of 0.5 µs. The tests were performed using the same projectiles as in the SHPB tests.

Quasi-static tests

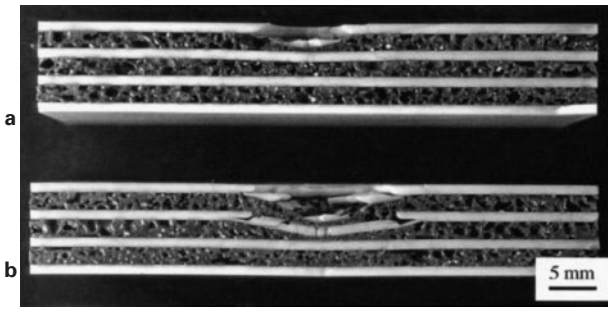
Quasi-static tests were carried out in order to compare the response with that of the low velocity impact tests. The tests were conducted using the same specimen, support, and indenter geometry as were employed in the low velocity impact tests. The indenter was fixed to the crosshead of a servohydraulic testing machine and the displacement rate was set at 2×10^{-5} m s⁻¹.

Damage assessment

Post-impact damage was assessed using X-ray radiography. Because of difficulties involved in determining the delamination area and the location at each interface, an overall area of damage, as viewed from the top, was estimated. Additionally, cross-sections of selected specimens were examined by optical and scanning electron microscopy, in order to identify the damage mechanisms that took place around the impact area.

Table 1 Summary of main properties of Al-12Si-0.6Mg foam used in fabrication of layered structures

Porosity, %	Compressive strength (20% strain), MPa	Tensile strength, MPa	Flexural strength, MPa
76 ± 3	7.2 ± 1.1	10.4 ± 2.0	9.7 ± 2.1



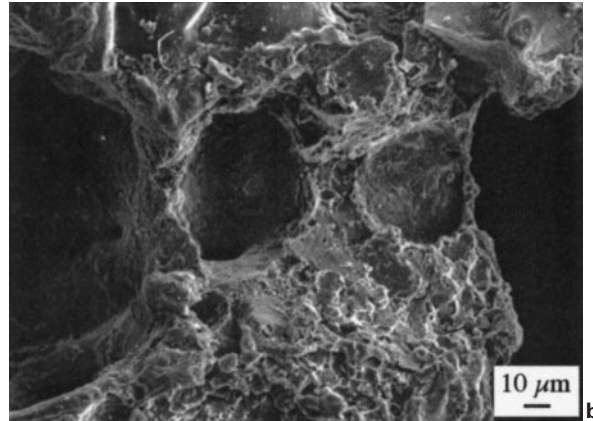
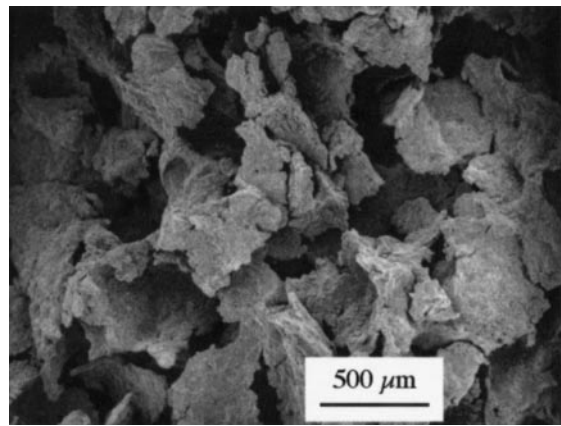
a 1.23 m s⁻¹; b 1.95 m s⁻¹

3 Diametric cross-sections of partially penetrated targets impacted at given velocities

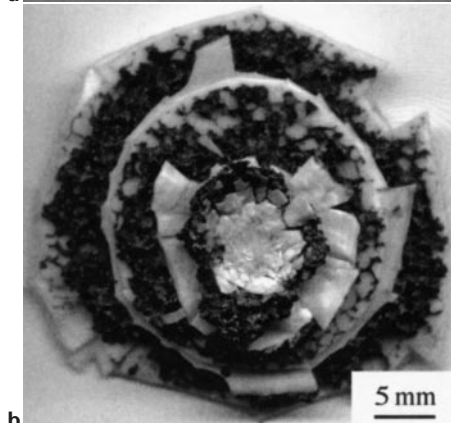
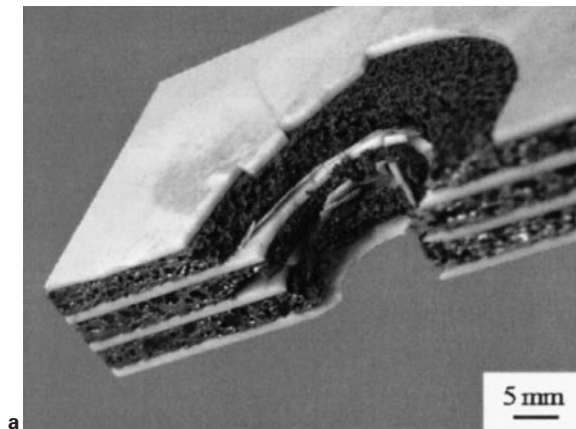
Results and discussion

LOW VELOCITY IMPACT

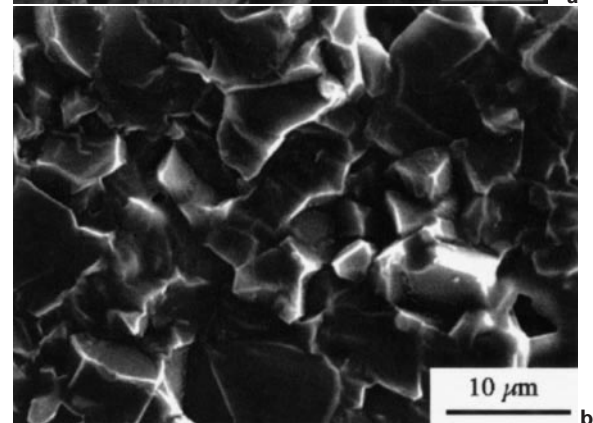
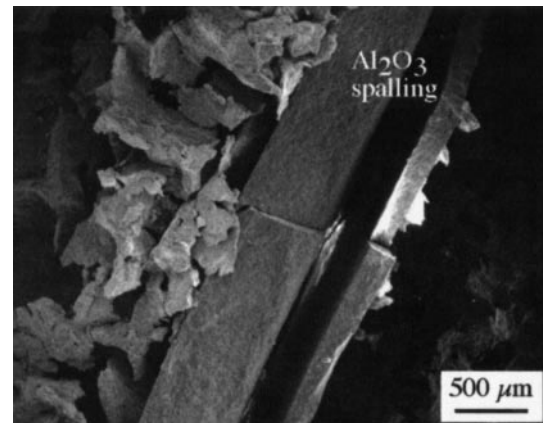
The laminates were impacted at different velocities, producing increasing damage up to penetration. Figure 3 shows cross-sections of two partially penetrated targets. At an impact velocity of 1.23 m s⁻¹ (Fig. 3a), the impactor fragmented the Al₂O₃, forming a network of radial cracks, crushed the foam beneath, and initiated damage in the next Al₂O₃ layer. At an impact velocity of 1.95 m s⁻¹, the impactor caused damage to a depth of about half the laminate thickness (Fig. 3b). At both velocities, the rear face of the targets suffered no damage. Also, indentation occurred with almost no evidence of out-of-plane deformation of the top Al₂O₃ layer (no radial cracks were found in the vicinity of the impact area). At higher impact velocities (2.75 m s⁻¹), the impactor pierced the laminate, and a distinctive plug



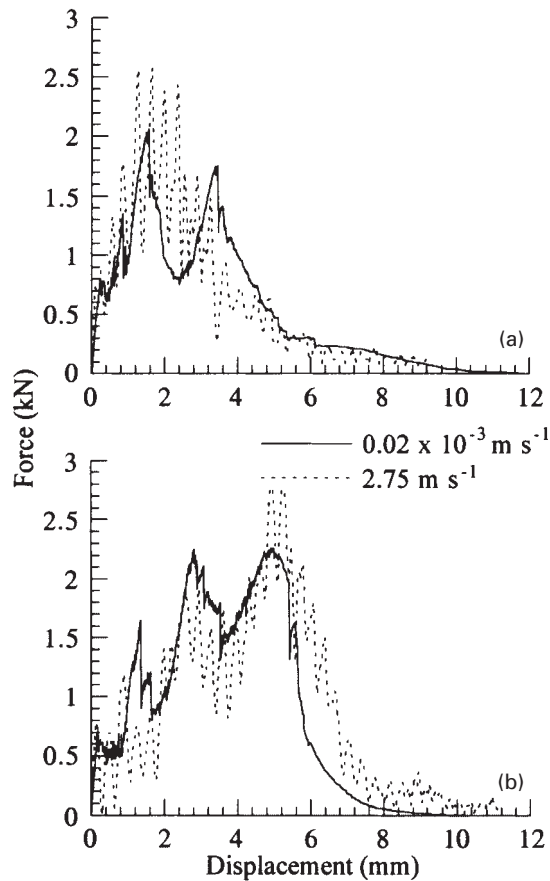
5 Micrographs (SEM) showing a foam macrostructure induced after penetration and b fractured cell wall



4 a penetrated target and b plug ejected



6 Micrographs (SEM) showing a Al₂O₃ spalling at periphery of penetrated zone and b Al₂O₃ fracture surface

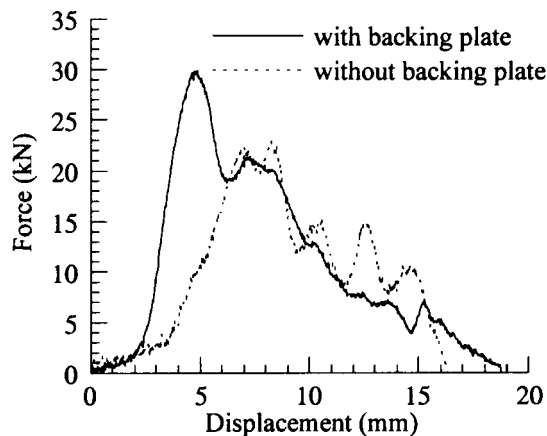


a $h_f=2$ mm; *b* $h_f=3$ mm

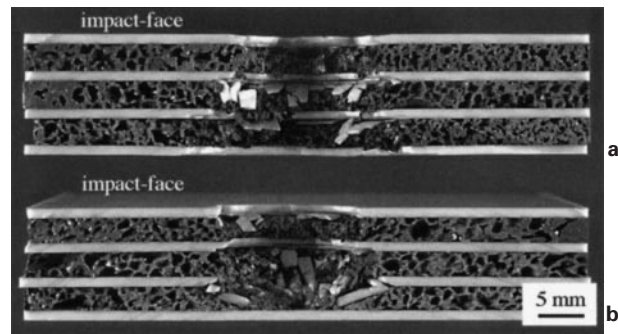
7 Comparison between static and low velocity impact responses for penetrated laminates with given foam layer thicknesses h_f

was ejected. Figure 4 shows a penetrated target and the plug detached by the impactor. The plug was almost conical in shape. From the side view of the plugs, it is inferred that the specimens, being relatively thick, do not respond immediately by flexing. In the early stages of impact, the target suffers mostly compressive failure in the contact region and, as the impactor moves further, deformation is replaced by a flexural failure mode. Local bending stresses in the Al_2O_3 layers are responsible for the residual curvature observed in the plugs.

The macrostructure of the Al alloy foam at the periphery of the penetrated zone (Fig. 5a) shows that the impactor



8 Force-displacement curves for impacts on thin laminates with and without backing plate: $h_f=2$ mm



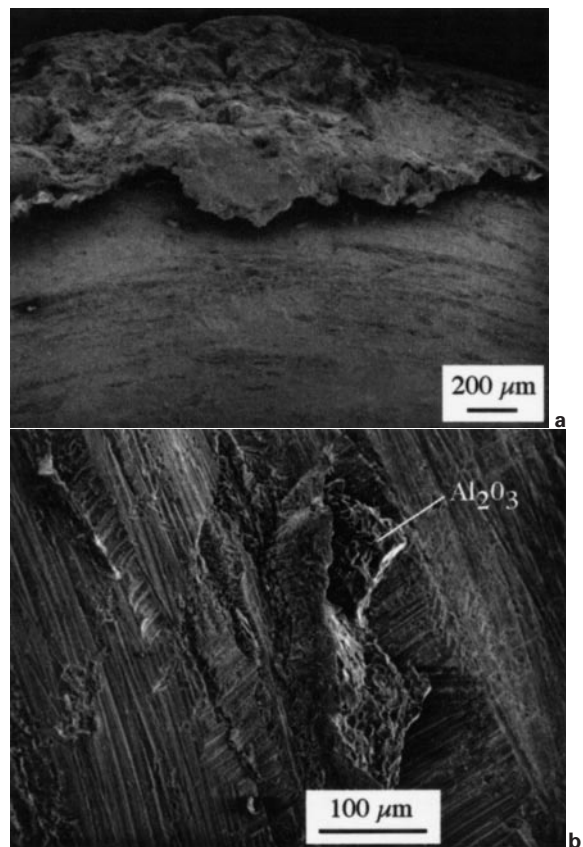
9 Diametric cross-sections of impacted laminates *a* without and *b* with backing plate

deforms the foam cell walls sideways as it pierces the laminate. Observation of the foam fracture surface reveals that failure occurs in a brittle manner, as indicated by the cleavage surface shown in Fig. 5b.

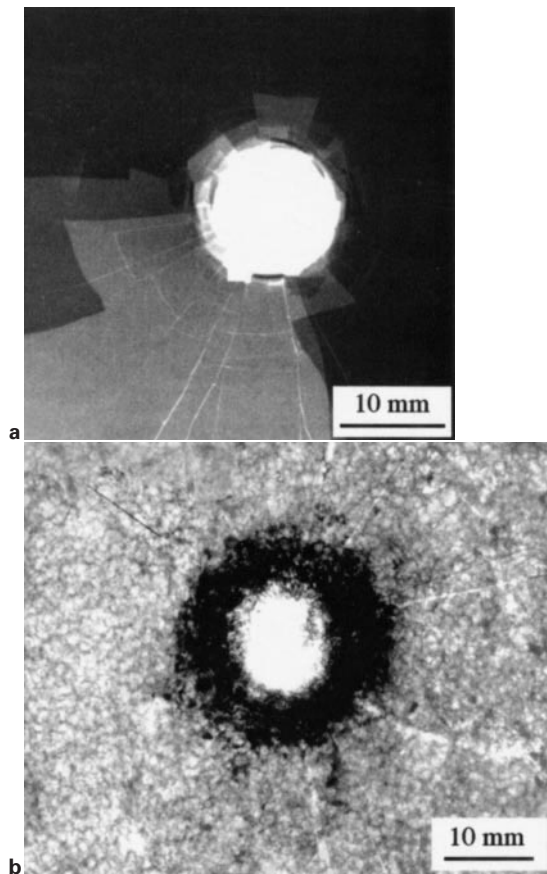
Side views of the penetrated laminates, such as those in Figs. 4 and 6a, reveal that the Al_2O_3 layers experience intense spalling. Spalls were consistently observed at the exit side of each Al_2O_3 layer and are attributed to in-plane tensions induced by bending. Investigation of the fracture surface of Al_2O_3 reveals a mixture of transgranular and intergranular failure, with the fracture mode being primarily intergranular (Fig. 6b).

LOW VELOCITY IMPACT VERSUS QUASI-STATIC

A commonly raised issue is whether low velocity impact can be rated as a quasi-static process. The most direct way of checking this assumption is by comparing the two



10 Micrographs (SEM) showing erosion of projectile: fragment of crushed Al_2O_3 powder is shown on surface of projectile in *b*



11 X-ray radiographs showing *a* dense metal laminate impacted at $\sim 200 \text{ m s}^{-1}$ (gas gun) and *b* back supported foam laminate impacted at $\sim 60 \text{ m s}^{-1}$ (Hopkinson bar)

responses. Figure 7 shows the static and low velocity impact response for laminates with two different foam layer thicknesses. Correspondence between the two curves is reasonably good. A noticeable difference between the two responses is that under dynamic loading the measured force exhibits pronounced oscillations. These oscillations have a relatively high frequency (10 kHz) and have been attributed to the fact that the impactor tup was loose and started vibrating against the load cell. The energy absorbed by the laminates, estimated by integrating force over distance, was similar in both the static and dynamic case. In particular, falling weight tests gave average energy absorption values of 6.3 and 9.5 J for the thin and thick laminates, respectively. These values are close to the statically measured ones (6.3 and 9.1 J, respectively). The mechanism of penetration was also similar for the two types of test.

Table 2 Gas gun results for Al–12Si foam/ Al_2O_3 laminates

Foam layer thickness, mm	Total thickness, mm	Areal density, kg m^{-2}	Striking velocity, m s^{-1}	Residual velocity, m s^{-1}	Absorbed energy, J
2.0	10.0	19.5	192.6	171.5	138.2
3.0	13.0	21.4	190.1	157.8	202.2

Table 3 Gas gun results for dense Al–12Si/ Al_2O_3 laminates

Metal layer thickness, mm	Total thickness, mm	Areal density, kg m^{-2}	Striking velocity, m s^{-1}	Residual velocity, m s^{-1}	Absorbed energy, J
0.5	5.6	19.3	192.0	176.7	101.5
0.8	6.4	21.4	187.4	171.4	103.3

SPLIT HOPKINSON PRESSURE BAR TESTS

Figure 8 shows representative force–displacement curves recorded for laminates impacted at $\sim 60 \text{ m s}^{-1}$. One of the curves corresponds to a laminate back-supported on a steel plate to prevent it from flexing. The backing plate induces rebound of the projectile and consequently increases the force transmitted. On the rear face of the target, radial cracks were formed. The cracks were centred beneath the impact zone and reached the laminate boundaries. No damage to the support plate was detected.

Unlike low velocity impact and static tests, complete piercing of the laminate by the impactor did not lead to the formation of a plug. The material pushed out by the impactor disintegrated into small fragments of various sizes. This generated a large fracture area, giving rise to an increase in the absorbed energy (*see* section on ‘Energy absorption per unit volume’ below). Moreover, impact at this velocity yielded a highly localised damage area. Localisation of damage may correlate with the fact that there was limited time available for the impact force to be dispersed over a broader area. (The contact time between the impactor and the laminates was $\sim 0.2 \text{ ms}$, compared with 3 ms in the drop weight tests.) Figure 9 shows side views of the penetrated targets with and without backing plate.

Because the Al_2O_3 layers were harder than the projectile material (steel), some projectile erosion occurred (Fig. 10*a*). Interaction between the projectile and the crushed Al_2O_3 powder caused the erosion strength of the projectile to be exceeded, leading to plastic deformation. As revealed in Fig. 10*b*, Al_2O_3 fragments were deposited on the projectile.

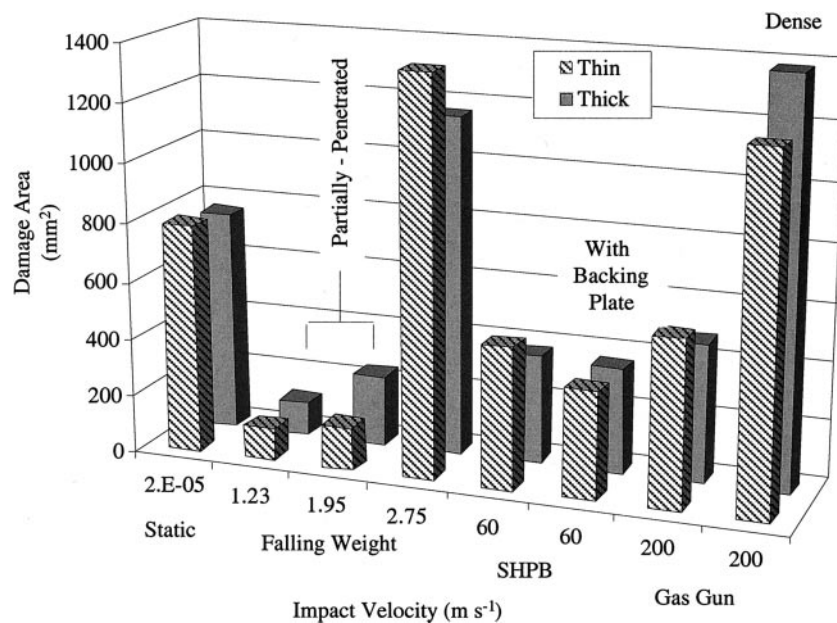
GAS GUN TESTS

The impact performance of foam laminates was compared with that of dense metal laminates of the same composition and areal density. The tests were carried out only once, and hence the associated conclusions must be regarded as tentative. The results are presented in Tables 2 and 3. Interestingly, the results suggest that the foam laminates are able to absorb more energy than dense laminates. The deformation pattern of the former is similar to that observed in the SHPB tests.

The fracture pattern of the dense metal laminates was rear-side cratering. The metal layers bulged in the direction of the projectile path. Furthermore, substantial debonding over the laminate thickness was evident (*see* section on ‘Quantification of damage’ below).

QUANTIFICATION OF DAMAGE

Since precise quantification of the delamination areas at each interface was extremely difficult, the projected damage area was determined using X-ray radiography. Two representative radiographs are shown in Fig. 11. Figure 11*a*



12 Damage area v. impact velocity for impacts on foam laminates: results for dense metal laminates impacted at $\sim 200 \text{ m s}^{-1}$ are also shown

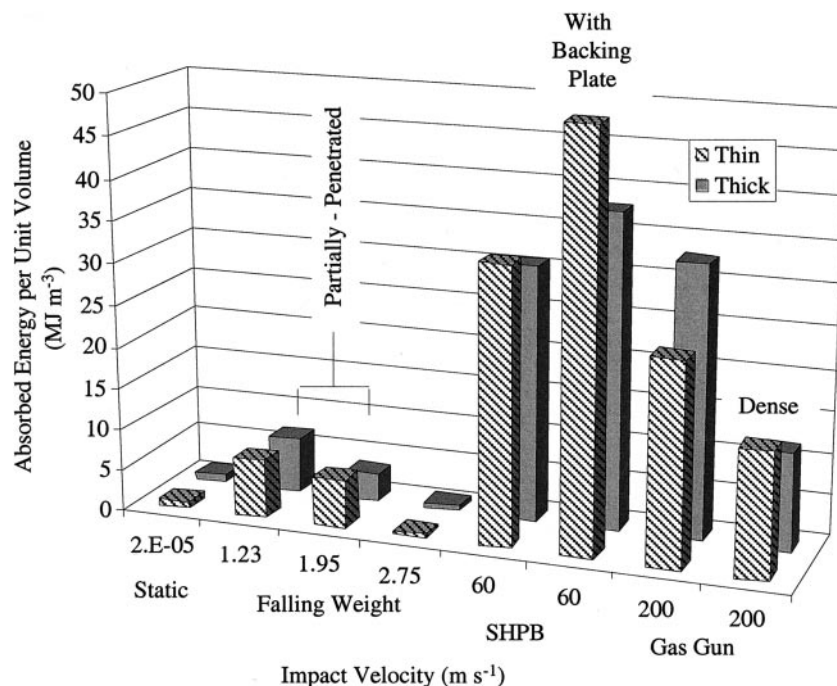
shows that piercing of the dense metal laminates produced debonding at different interfaces (changes in the blackening of the film) and also radial and circumferential cracking in the Al_2O_3 layers. In the case of foam laminates (Fig. 11b), a radio-opaque penetrant was used to aid the detection of the delaminated area. Note that radiography cannot detect foam crushing. Figure 11b shows an annular damaged area caused by Al_2O_3 spalling. Also, radial cracks propagating towards the edges of the specimen are evident.

The projected delamination area and size of penetration were measured for all the impacted specimens and the results are summarised in Fig. 12. The figure shows that under static and low velocity impact conditions, the impactor causes a more global deformation of the foam

laminates. By contrast, under intermediate velocity impacts (Hopkinson bar and gas gun tests), the laminate response is more localised.

ENERGY ABSORPTION PER UNIT VOLUME

For fully penetrated laminates, energy absorption per unit volume of damaged material has been calculated by dividing the energy by the product of damage area and laminate thickness. For partially penetrated laminates, the energy has been divided by the product of damage area and indentation depth. Because the damage area was determined by projecting damage areas at all interfaces onto a single plane, the results summarised in Fig. 13 represent



13 Energy absorption per unit volume v. impact velocity for impacts on foam laminates: results for dense metal laminates impacted at $\sim 200 \text{ m s}^{-1}$ are also shown

lower bounds. The results suggest that under intermediate velocity impacts (SHPB and gas gun tests), foam laminates absorb more energy per unit volume than under static and low velocity impact conditions. This is chiefly owing to a substantial increase in energy absorption caused by a change in the penetration mode from plugging to fragmentation, and only partly owing to localisation of damage. In addition, foam laminates are found to absorb more energy than dense metal laminates of the same composition and areal density under conditions of enforced crushing (gas gun results from Tables 2 and 3).

Conclusions

An experimental study has been carried out to characterise the impact response of metallic foam/ceramic laminates in low and intermediate velocity ranges. The main conclusions are outlined below.

1. There is good correlation between the low velocity impact and static responses.
2. Under low velocity impact and static conditions, the impactor induces more global deformation of the laminates. By contrast, impact at higher velocities yields highly localised damage.
3. Increasing impact velocity causes a change in the failure mode from plugging to fragmentation. This is accompanied by a pronounced increase in energy absorption.
4. Preliminary results at high impact velocities ($\sim 200 \text{ m s}^{-1}$) suggest that foam laminates are able to absorb more energy than dense laminates of the same composition and areal density.

Acknowledgements

Thanks are due to the State Scholarships Foundation of Greece for financial support for one of the authors (AEM), to Dr F. Simancik and Dr J. Kovacik (SAS, Slovakia) for providing the metallic foam, to Mr A. Foreman and Dr R. White (DERA Farnborough, UK) for performing the impact tests. Also, the authors are grateful to Professor T. Wierzbicki (MIT, USA) for useful discussions.

References

1. D. SHERMAN and D. G. BRANDON: *J. Mater. Res.*, 1997, **12**, 1335–1343.
2. F. K. KO, A. J. GESHURY, and J. W. SONG: Proc. 11th Int. Conf. on 'Composite materials' (ICCM-11), Gold Coast, Queensland, Australia, July 1997, (ed. M. L. Scott), Vol. 2, 464–473; 1997, Leatherhead, Woodhead.
3. F. K. KO and J. CHANG: Proc. 12th Int. Conf. on 'Composite materials' (ICCM-12), Paris, France, July 1999, (ed. T. Massard and A. Vautrin), Société Française de Métallurgie et de Matériaux, Paper 1358.
4. A. HAQUE, A. ABUTALIB, K. RAHUL, U. K. VAIDYA, H. MAHFUZ, and S. JEELANI: Proc. 12th Int. Conf. on 'Composite materials' (ICCM-12), Paris, France, July 1999, (ed. T. Massard and A. Vautrin), Société Française de Métallurgie et de Matériaux, Paper 481.
5. F. SIMANCIK, H. P. DEGISCHER, and H. WÖRZ: Proc. 4th European Conf. on 'Advanced materials and processes' (Euromat '95), Venice/Padua, Italy, 1995, Associazione Italiana di Metallurgia, 191–196.

POLYMER PROCESS ENGINEERING 99

Edited by

P. D. Coates

Book 721 ISBN 1 86125 094 0 Hbk

European Union £40/Members £32

Non-European Union \$80/Members \$64

p&p European Union £5.00/Non-EU \$10.00 per order

Orders to: IOM Communications Ltd, Shelton House, Stoke Road, Shelton,
Stoke-on-Trent ST4 2DR Tel: +44 (0) 1782 202 116 Fax: +44 (0) 1782 202 421
Email: Orders@materials.org.uk Internet: www.materials.org.uk



IOM Communications

VAT Registration No. GB 649 1646 11 Reg. Charity No. 1059475

IOM Communications Ltd is a wholly owned subsidiary of the Institute of Materials